Soft Matter

PAPER

View Article Online
View Journal | View Issue

Cite this: *Soft Matter*, 2016, **12**, 1192

Construction of a smart temperature-responsive GPx mimic based on the self-assembly of supra-amphiphiles†

Huixin Zou, Hongcheng Sun, Liang Wang, Linlu Zhao, Jiaxi Li, Zeyuan Dong, Quan Luo, Jiayun Xu and Junqiu Liu*

Glutathione peroxidase (GPx) is a major defense against hydroperoxides as a kind of seleno-enzyme that protects cells from oxidative damage. A supramolecular vesicle with controllable GPx activity and morphology has been successfully constructed by the self-assembly of supra-amphiphiles formed by host–guest recognition between cyclodextrin and adamantane derivatives. By introducing thermosensitive poly(*N*-isopropylacrylamide) (PNIPAM) scaffolds and the catalytic moiety selenium into adamantane and cyclodextrin, respectively, the complex of catalysis-functionalized cyclodextrin with thermosensitivity-functionalized adamantane directed the formation of a supramolecular vesicle which acted as a GPx mimic at 37 °C. The self-assembled nanoenzyme exhibited an obvious temperature responsive characteristic and high GPx-like catalytic activity promoting the reduction of hydrogen peroxide (H_2O_2) with glutathione (GSH) as the reducing substrate at 37 °C. However, the vesicle disassembled when the temperature decreased to 25 °C due to the transition of PNIPAM between the coil and the globule. Interestingly, the catalytic activity changed along with the transformation of morphologies. The vesicle structure self-assembled at 37 °C provided the favorable microenvironment for the enzymatic reaction, hence we successfully developed a temperature-responsive nanoenzyme model. Moreover, the catalytic activity of the thermosensitive GPx mimic exhibited excellent reversibility and typical saturation kinetics behaviour similar to a natural enzyme catalyst. It is assumed that the proposed GPx model not only has remarkable advantages such as easy functionalization and facile preparation but also provided a new way to develop intelligent responsive materials.

Received 19th August 2015,
Accepted 17th November 2015

DOI: 10.1039/c5sm02074c

www.rsc.org/softmatter

Introduction

Enzymes, serving as a class of highly specific and efficient biocatalysts in nature, enhance the rates of reactions between the metabolites *in vivo*. The design of artificial enzymes represents one of the increasingly significant topics in the research of biomaterials. Reactive oxygen species (ROS), which are produced by the cellular metabolic process, play an essential role in cell signaling.[1] They are friendly to the living organisms in general, nevertheless, the release of surplus ROS may also result in oxidative damage and eventually some diseases, such as neuronal apoptosis, cardiovascular diseases and inflammatory processes.[2,3] Glutathione peroxidase (GPx) (EC 1.11.1.9) is a crucial selenoenzyme involved in scavenging ROS by catalyzing the reduction of hydroperoxides (ROOHs) using glutathione (GSH) as a reducing substrate.[4,5] It is apparent that mimicking the excellent antioxidation performance of natural GPx without the intrinsic disadvantages is of vital importance. On the other hand, building reliable artificial GPx models in a smart manner remains challenging and significant. In chemists' hands, remarkable accomplishments have been obtained by introducing selenium catalytic centers into the substrate-binding scaffolds, including chemical and biological modifications. In particular, in the case of some chemical methods, seleno-dendrimers[6] and selenium- or tellurium-containing interactional small organic compounds[7,8] are typical examples. In recent years, our group has focused on the construction of highly efficient selenium-containing enzymes based on the understanding of the structure of a native GPx by the incorporation of catalytic centers with existing or artificially generated scaffolds.[9–13]

Achievements in supramolecular chemistry provide strong incentives to construct artificial enzymes. However, establishing an activity-controllable nanoenzyme system has become an overarching goal in the design of smart artificial enzymes. To meet the challenge, stimulus-responsive architectures with chemical

State Key Laboratory of Supramolecular Structure and Materials, College of Chemistry, Jilin University, Changchun 130012, People's Republic of China. E-mail: junqiuliu@jlu.edu.cn; Fax: +86-431-85193421

† Electronic supplementary information (ESI) available. See DOI: 10.1039/c5sm02074c

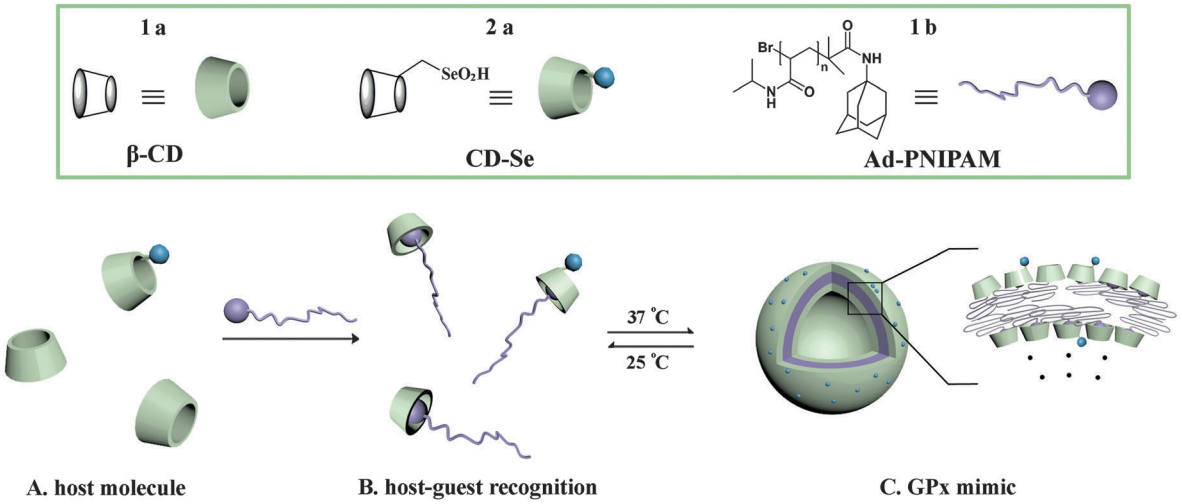

Scheme 1 Schematic representation of the self-assembly process based on host–guest recognition and the temperature responsive behaviour of the GPx mimic.

triggers[14,15] have been designed to provide the capability to control the catalytic activity of GPx mimics. In the meanwhile, the intelligent analogues of enzymes in response to a variety of factors have attracted growing attention, such as thermal,[16] photoresponsive,[17] redox[18] and even mechanical forces.[19] Among these stimulus-responsive artificial enzymes, poly(*N*-isopropylacrylamide) (PNIPAM), acting as a smart material, has been widely investigated due to its thermal responsive properties. Owing to its transition between the coil and the globule upon temperature changes, PNIPAM presents a dramatic phase transition in water. The temperature related to conformational changes is defined as the lower critical solution temperature (LCST).[20–22] When the temperature is below the LCST, the PNIPAM block is hydrophilic whereas hydrophobic above the LCST.[23] Compared to other thermal responsive nanomaterials, the unique change in the physical properties of PNIPAM has received much attention from researchers in fabricating thermal responsive assemblies. To the best of our knowledge, the self-assembly by host–guest recognition has been investigated as an effective tool to construct functional nanostructures in aqueous media with broad application prospects.[24–28] In addition, vesicles, fibers or nanotubes constructed by the assembly of amphiphiles are not only common building blocks in living systems but also fundamental components of artificial biomimetic systems, molecular imprinting systems, microreactors, and especially drug delivery systems.[13,29] Herein, we designed a supra-amphiphilic thermosensitive vesicle-like structure by the self-assembly of host–guest interaction between cyclodextrin (CD) and adamantine (Ad) derivatives to construct a novel artificial GPx mimic with controllable catalytic activity. Specifically, Ad-headed PNIPAM (Ad-PNIAM, Scheme 1, **1b**) served as the guest molecule while cyclodextrin-based selenic acid (CD-Se, Scheme 1, **2a**) acted as the host in this complex. At 25 °C, the host–guest complexation events occurred in aqueous solution and the PNIPAM chains had high-solubility below the LCST, meanwhile the complex became hydrophilic and the selenium catalytic centers were distributed randomly in water solution, which resulted in a relatively low catalytic efficiency. Whereas with the chains becoming coiled at 37 °C, the polymer turned hydrophobic, thus leading to the formation of a supra-amphiphilic molecule. It further self-assembled into vesicles and the selenium catalytic centers were aggregated and exposed on the surface. The supra-amphiphilic vesicles might thus offer an outstanding model for fabricating a GPx mimic with high catalytic activity by centralizing the catalytic centers together (Scheme 1). Furthermore, the catalytic activity of this smart artificial GPx mimic can be reversibly modulated by temperature.

Materials and methods

Materials

N-Isopropylacrylamide (NIPAM) was purchased from Sigma-Aldrich and recrystallized from the mixture of toluene and hexane with a proportion of 3 : 7. Tris(2-dimethylaminoethyl)-amine (Me_6TREN), glutathione reductase (GR), glutathione (GSH) and β-nicotinamide adenine dinucleotide phosphate (NADPH) were purchased from Sigma-Aldrich and used directly. Sodium borohydride ($NaBH_4$) and H_2O_2 were purchased from Sinopharm Chemical Reagent Co. Ltd and were used without further purification. Cuprous bromide (CuBr) was synthesized from cupric bromide ($CuBr_2$) and sodium sulfite (Na_2SO_3). Selenium powder, 4-toluene sulfonyl chloride (PTSC) and β-cyclodextrin were purchased from Aladdin Industrial Corporation, among which β-cyclodextrin was recrystallized three times before use. Milli Q water was used in the assembly process and other solvents were of analytical grade.

Instruments and measurements

A Bruker Advance 500 (500 MHz) ^{1}H NMR spectrometer was employed to characterize the structures of the compounds. Molecular weights were determined by MALDI-TOF, ESI-MS spectrometric analyses and GPC. Scanning electron microscopy

(SEM) observations were carried out on a JEOL FESEM 6700F scanning electron microscope where the primary electron energy is 3.00 kV. Transmission electron microscopy (TEM) observations were carried out using a JEM-2100F scanning electron microscope. The UV-vis spectroscopy spectrum was supervised using a Shimadzu 2450 UV-VIS-NIR spectrophotometer. And a Malvern Zetasizer NanoSeries instrument was used to monitor the size of the vesicle.

Synthesis of the initiator compound 1

Amantadine (1.0 g, 6.6 mmol) and desiccative trimethylamine (1.8 mL, 13.2 mmol) were dissolved in 20 mL of anhydrous dichloromethane in a 100 mL round flask. 2-Bromoisobutyryl bromide (0.8 mL, 6.6 mmol) was dissolved in 10 mL of anhydrous dichloromethane and added dropwise to the aforesaid round flask in an ice-bath and stirred for 12 h. The solution was then extracted from water and dichloromethane. The organic phase was collected and the resulting product was purified by column chromatography (silica gel, dichloromethane). Yield: 85%. ^{1}H NMR (500 MHz, $CDCl_3$) δ 2.15–2.10 (3 H, –CH–), 2.05 (6 H, –CH_2–), 1.74–1.70 (6 H, –CH_2–), 1.95 (6 H, –CH_3).

Synthesis of Ad-PNIPAM (2)

Ad-PNIPAM was synthesized according to the polymerization procedure reported by Masci *et al.*[30] NIPAM (848.0 mg, 7.5 mmol), Me_6TREN (23.0 mg, 0.1 mmol), and DMF (5.0 mL) were introduced into a Schlenk tube equipped with a magnetic bar and an oil bath followed by three freeze–pump–thaw cycles. And then, CuBr (14.4 mg, 0.1 mmol) was added under nitrogen followed by two freeze–pump–thaw cycles. Finally, initiator compound **1** (30.0 mg, 0.1 mmol) was deoxygenized and added to the Schlenk tube *via* a syringe to start the polymerization. The mixture was stirred for 48 h at 60 °C. The mixture was then exposed to air to terminate the polymerization and the solution was dialyzed against water for 3 days. The resulting solution was freeze-dried using a lyophilizer (Scheme 2a). ^{1}H NMR analysis of the polymer revealed a ratio of NIPAM : Ad of 65 : 1 (Fig. S5, ESI†). The GPx mimic showed high activity and was provided with excellent temperature-responsive effects at this ratio.

Synthesis of CD-Se (4)

6,6′-Selenium bridged bis-6-deoxy-β-cyclodextrin (6-CD-SeSe-CD, **3**) was prepared as described previously except that tellurium powder was replaced by selenium powder.[31] 6-CD-SeSe-CD (100.0 mg, 0.04 mmol) was dissolved in Milli Q water (20 mL), and then a large excess amount (30%, 200 μL) of H_2O_2 was added in an ice-bath and stirred overnight. The resulting product was purified by Sephadex G-15 column chromatography with Milli Q water as the eluent (Scheme 2b). A white solid product **4** was obtained by freeze-drying (41.6 mg, 0.03 mmol, 80%).

LCST determination of Ad-PNIPAM

The determination of LCST of Ad-PNIPAM was carried out according to the previously reported recipes.[32] We measured the optical transmittance of the Ad-PNIPAM solution (0.1 mM, pH = 7, PBS) at 600 nm using a Shimadzu 2450 UV-VIS-NIR spectrophotometer at different temperatures from 25 °C to 45 °C. The LCST of PNIPAM-CD was found to be 32.4 °C.

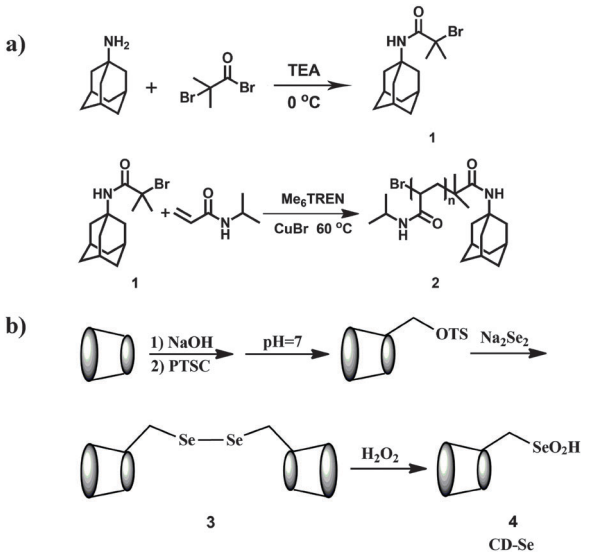

Scheme 2 Synthetic route of (a) Ad-PNIPAM and (b) CD-Se.

Preparation of GPx mimics

β-CD, CD-Se and Ad-PNIPAM were dissolved in DMF at a concentration of 20 mM in three Eppendorf tubes, mixed them together at a ratio of 4 : 1 : 5, and sonicated for 20 min to get the complex in high concentration (10 mM) at 25 °C (below the LCST of Ad-PNIPAM). The stock solution was diluted with Milli-Q water to a final concentration of 0.1 mM and the temperature was raised to 37 °C which was above the LCST of NIPAM. The above solution was sonicated for 20 min to prepare the GPx mimics and the opalescence appeared.

LCST determination of the assembled complex

The same method as that of Ad-PNIPAM was carried out to detect the optical transmittance of the assembled complex (PBS, 0.1 mM, pH = 7) solution at different temperatures. And the LCST of the assembled complex was 33.2 °C. Compared with the GPx mimic, the LCST of the complex which was comprised of Ad-PNIPAM and β-CD was found to be 33.4 °C.

Determination of GPx catalytic activity

GPx activity was determined using H_2O_2 and GSH as substrates on the basis of the previous method reported by Wilson[33] (see the following chemical equation).

$$2GSH + H_2O_2 \xrightarrow{\text{Enzyme}} GSSG + H_2O$$

$$GSSG + NADPH + H^+ \xrightarrow{\text{Glutathione reductase}} 2GSH + NADP^+$$

The reaction was carried out at 37 °C in a 500 μL quartz cuvette of phosphate buffer (pH = 7.0, 50 mM) containing 1 mM GSH, 1 mM EDTA, 1 unit of glutathione reductase and 0.01 mM GPx mimic (calculated based on the concentration of selenium). In this coupled reductase assay system, heat is preserved for

3 min, and then 50 mL of NADPH (0.25 mM) was added. The mixture was preincubated for 3 minutes and the reaction was then initiated by the addition of 50 mL of H_2O_2 (0.50 mM). Since the UV spectrum of NADPH exhibits an intense absorption peak at 340 nm, the initial rates for the reduction of H_2O_2 by GSH would be expected to be determined by monitoring the absorption decrease of NADPH at 340 nm using a Shimadzu 2450 UV-VIS-NIR spectrophotometer. Appropriate control of the non-enzymatic reaction was assayed and subtracted from the catalyzed reaction.

Results and discussion

LCST behaviour

In our study, on account of the temperature responsive behaviour of the guest molecule, when the temperature exceeded the LCST, the soluble PNIPAM transformed into an insoluble polymer that served as the hydrophobic block, while CD performed the hydrophilic part. The complex showed excellent temperature-responsive behaviour and provided the platform to construct universal self-assembled materials.[34,35] Hence, it is a necessity to investigate the thermal-responsive properties of the polymer Ad-PNIPAM. The controllable structural change of PNIPAM can be realized by modulating the temperature of the complex. Fig. 1 shows the optical transmittance of the guest molecule Ad-PNIPAM (curve a) and the assembly (curve b) at different temperatures. The LCST of Ad-PNIPAM and the complex was 32.4 °C and 33.2 °C, respectively, which suggested that the introduction of hydrophilic CD and CD-Se with appropriate proportion as the nestable container for Ad-PNIPAM through host–guest interaction mildly changes the LCST. In all cases, it is clear that the polymer with temperature-responsive feature is able to control its own hydrophilic–hydrophobic properties by temperature.

Construction and characterization of the nanoenzyme

CD is a typical member of host family, which has a cavity and exhibits brilliant host–guest properties including encapsulating guest molecules inside to form a 1:1 complex.[36–41] Involving the host–guest complex formation between CD and an Ad-headed PNIPAM guest molecule, our process builds a novel supramolecular amphiphilic assembly. The CD moiety acted as the hydrophilic part while PNIPAM shrinked and served as the hydrophobic portion at 37 °C (above the LCST). This amphipathic molecule may focus intense effort on the further self-assembly. The morphology of the GPx mimic was characterized by scanning electron microscopy (SEM). As shown in Fig. 2A, the SEM image confirmed the existence of the spherical morphology of the GPx mimic at 37 °C with a diameter ranging from 200 to 400 nm. In contrast, the vesicular morphology could hardly be observed at 25 °C (Fig. S8, ESI†). It could be easily assumed that host–guest recognition has taken place and the complex was totally hydrophilic under these conditions at 25 °C, which restricted the further self-assembly.

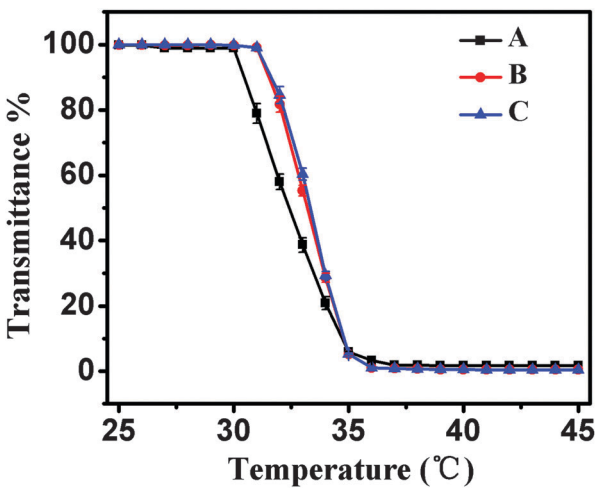

Fig. 1 Optical transmittance at 600 nm obtained for solutions (pH = 7.0, 50 mM PBS) of (A) Ad-PNIPAM, (B) GPx mimic and (C) complex of Ad-PNIPAM and β-CD at a concentration of 0.1 mM.

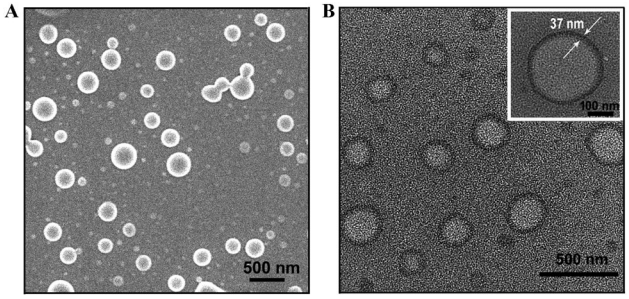

Fig. 2 (A) SEM image and (B) TEM image of the GPx mimic at 37 °C.

To further explore the detailed structure of the spherical assembly, TEM observation was carried out. Fig. 2B demonstrates a striking contrast between the periphery and the inner part of the spherical nanoparticles, which is a typical characteristic for hollow vesicles. And the wall thickness of the vesicle is about 37 nm. In comparison, TEM observation was also carried out on the guest molecule (Ad-PNIPAM) under the same conditions (Fig. S9, ESI†). It turned out that the morphology of the guest molecule was a solid micelle and the diameter was about 50 nm at 37 °C, which was different from the assemblies. All these results proved that we have successfully developed a vesicle-like GPx mimic. Moreover, we employed X-ray diffraction (XRD) (Fig. 3) to further offer detailed information about the layered structure of the vesicle. The thickness of each layer was calculated to be 1.45 nm according to the Bragg equation and the wall of the vesicle was composed of about 26 layers. The result of XRD is another powerful evidence for the formation of regular vesicle-like architectures and the preparation of the GPx mimic. The vesicle-like GPx mimic confirmed by SEM, TEM, and XRD was accumulated by many layers, therefore forming a well-ordered superstructure as shown in Scheme 1. The hydrophilic CD faced outside whereas the hydrophobic polymer chain shrinked interiorly.

The temperature dependence of the hydrodynamic diameters of the assemblies and the guest molecule was further characterized by dynamic light scattering (DLS). As shown in Fig. 4, the current soluble Ad-PNIPAM adopted an extended conformation and exhibited a diameter of about 10.1 (±1.0) nm at 25 °C.

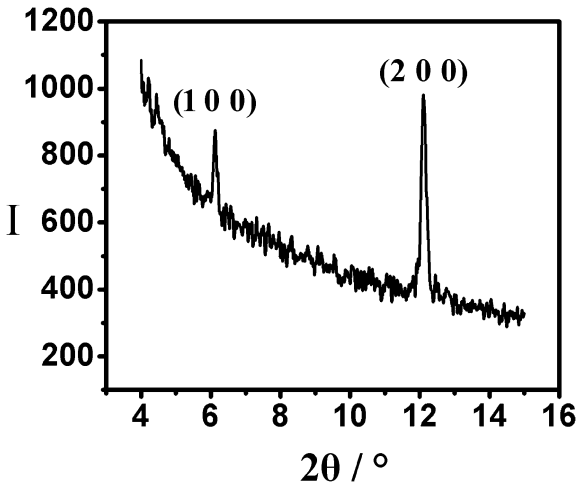

Fig. 3 XRD scan of the vesicle-like assemblies.

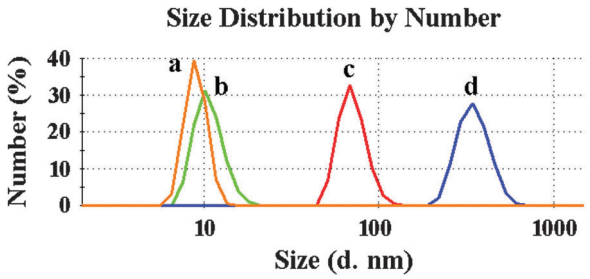

Fig. 4 The hydrodynamic diameters of Ad-PNIPAM (b and c) and GPx mimic (a and d) determined using a dynamic light scattering instrument, and the concentration of the sample was 0.1 mM in water. From (a) to (d), the temperature was 25 °C, 37 °C, 25 °C, and 37 °C, respectively.

When the temperature climbed to 37 °C (higher than the LCST), the chain aggregated and then self-assembled into micelles. As a result, the hydrodynamic diameters became 68.1(±3.5) nm (curve c). Nevertheless, with the addition of the host molecule CD, only host–guest recognition occurred at 25 °C (curve a, 8.7 (±0.5) nm) and an increase in temperature gradually led to the conformational change of PNIPAM, which further resulted in the formation of the supra-amphiphilic assemblies. The phenomena above were mainly reflected in the increase of hydrodynamic diameters (curve d, 342.0 (±18.0) nm) at 37 °C which was approaching to what we have observed in SEM images. All these results demonstrated that the temperature controlled amphipathic GPx mimic fabricated by supramolecular interactions was successfully constructed.

Catalytic behaviour of the GPx mimic

We modified selenium onto the host molecule CD by chemical modification to simulate the function of GPx in our well-designed architecture. The activity of the GPx mimic for the reduction of H_2O_2 by GSH was measured according to a coupled reductase assay system. The absorbance at 340 nm was registered to calculate the reaction rate on the basis of the decreased absorption value of NADPH. In our nanoenzyme model, by regulating the conformation of the thermosensitive polymer PNIPAM that linked to the guest molecule, the construction of the temperature-responsive GPx mimic was realized. To investigate the temperature responsive properties of the GPx mimic, the activity of the nanoenzyme was determined with the temperature ranging from 25 to 43 °C, and the activity values are shown in Table 1 and by plotting the catalytic activity against temperature, an optimum temperature curve was obtained (Fig. 5B). The corresponding blank experiments without mimic enzyme were also carried out to deduct the background. As the temperature increases to LCST, the catalytic activity increased slowly with low magnitude. However, it is noted that with increasing temperature further up to 37 °C, the activity values had a sharp promotion due to the formation of stable assemblies and the effect of the vesicle structure that provided the

Table 1 GPx activities of one catalytic center on supramolecular nanoenzymes for the reduction of H_2O_2 by GSH at pH 7.0 and various temperatures

Number	Catalyst	Temperature (°C)	ν_0[a] (μM min^{-1})
1	GPx mimic	25.0	1.3 ± 0.08
2	GPx mimic	28.0	3.0 ± 0.2
3	GPx mimic	30.0	4.9 ± 0.3
4	GPx mimic	32.0	5.7 ± 0.3
5	GPx mimic	34.0	6.9 ± 0.3
6	GPx mimic	35.0	9.7 ± 0.4
7	GPx mimic	37.0	19.9 ± 0.6
8	GPx mimic	39.0	18.6 ± 0.5
9	GPx mimic	41.0	17.3 ± 0.5
10	GPx mimic	43.0	17.2 ± 0.5
11	PhSeSePh[b]	25.0	0.03 ± 0.001
12	PhSeSePh[b]	37.0	0.2 ± 0.008

[a] The GPx activity was corrected for spontaneous reaction in the presence of the enzyme (2 μM) and assuming one molecule catalytic center (selenium moiety) as one active site of the enzyme. The thermosensitive nanoenzyme was constructed by **1a**, **2a** and **1b** (Scheme 1). [b] The concentration of catalyst PhSeSePh was 10 μM. All the results are means of at least three repeats.

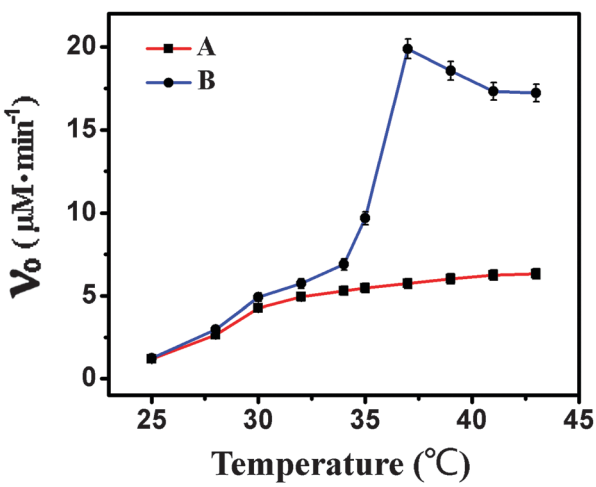

Fig. 5 Plots of the catalytic rate of (A) complex of Ad-PNIPAM, β-CD and Se-CD and (B) the GPx mimic *vs.* temperature during the catalytic reduction of H_2O_2 (0.5 mM) by GSH (1 mM) with catalytic center 2.00 μM. The range of temperature is from 25 to 43 °C.

favorable environment for catalytic reaction. Subsequently, the catalytic activity decreased slightly when the temperature further increased above 37 °C, which demonstrated that 37 °C was found to be the optimal temperature for our GPx mimic. The real-time catalytic plots of absorbance *versus* time during the catalytic reduction are displayed in the ESI† in Fig. S10. On the one hand, increasing the temperature results in the conformational change of PNIPAM and the occurrence of the amphiphilic self-assembly, in which case the assemblies were proved to be vesicle structures and the active site Se was gathered and exposed to the substrates, efficiently facilitating the binding between the substrates and the catalytic centers. On the other hand, owing to the unique structure of the supramolecular amphiphilic nanoenzyme, the catalytic capability in each catalytic center presents a remarkable promotion. As expected, the vesicle-like GPx mimic exhibited a relatively high catalytic activity (19.9 ± 0.6 μM min^{-1}) at 37 °C. In contrast, at 25 °C the complex showed rather low catalytic activity (1.3 ± 0.08 μM min^{-1}) (Table 1). Moreover, we prepared a non-responsive version to form supramolecular complexes as a contrast experiment and plotted the catalytic activity *versus* temperature to obtain a contrastive temperature curve under homogeneous conditions (Fig. 5A). By replacing PNIPAM with PEG-5000, the contrastive supramolecular complexes comprising Ad-PEG, CD and CD-Se were completely hydrophilic when the temperature increases from 25 °C to 43 °C. Thus the catalytic activity of complexes increased slowly as temperature moved up and the maximum value only reached 6.3 ± 0.3 μM min^{-1}. Compared with our GPx mimic, this result sufficiently demonstrated that the well-designed artificial GPx mimic exhibited outstanding catalysis ability. Furthermore, the catalytic rate (see Table 1) of our well-designed GPx mimic showed two orders of magnitude bigger than PhSeSePh under the identical conditions and exhibited considerable higher catalytic activity. Meanwhile, refer to the catalytic activities that were reported for the other systems.[42–44] It was remarkable that our GPx mimic proved at least two orders of magnitude larger than the maximum catalytic rate of the selenium containing catalysts in their systems (Table S1a and b, ESI†). The maximum catalytic rate of our GPx mimic was determined to be similar to other artificial enzymes (Table S1c, ESI† SGPx). However, SGPx was modified to contain three catalytic elements (catalytic center), whereas our GPx mimic has been modified to contain only one catalytic element. At this point, our artificial selenium enzyme has been perceived as an excellent GPx mimic with reasonably high catalytic activity.

Furthermore, we studied the saturation kinetics of the GPx mimic in peroxidase-like reaction at individual concentrations of the substrate H_2O_2 to find out that the nanoenzyme fitted the typical saturation kinetics and exhibited real catalytic behaviour (Fig. 6). In the coupled reductase assay system, in the presence of the GPx mimic (2.0 μM catalytic center) at 37 °C and pH = 7.0, according to the Michaelis–Menten equation, the apparent kinetic parameters of the GPx mimic were acquired as $K_{mGSH}^{(app)}$ = 391.98 M, $k_{cat}^{(app)}$ = 18.97 min^{-1} and $k_{cat}^{(app)}/K_{mGSH}^{(app)}$ = 4.84×10^4 μM^{-1} min^{-1} and the turnover number per catalytic center of selenium was calculated to be 19 min^{-1}. This was taken as proof that we have built a real enzyme mimic. Based on a

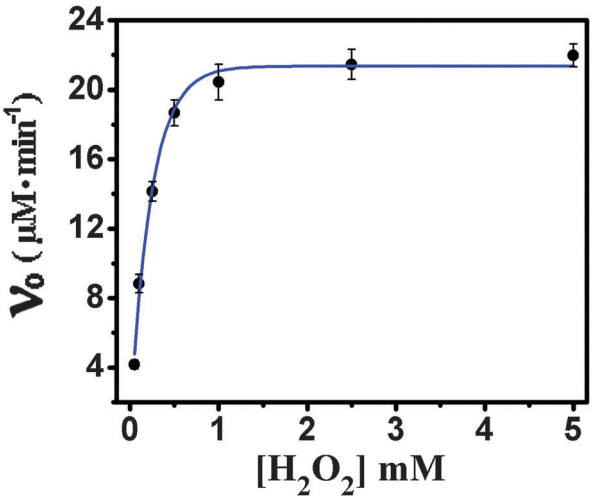

Fig. 6 Plot of the initial rate at different concentrations of H_2O_2 in the presence of the GPx mimic (2.0 μM catalytic center) at pH = 7.0 (50 mM PBS). The initial concentration of GSH was fixed to 1 mM. The concentrations of H_2O_2 were 0.05 mM, 0.1 mM, 0.25 mM, 0.5 mM, 1.0 mM, 2.5 mM and 5 mM, respectively.

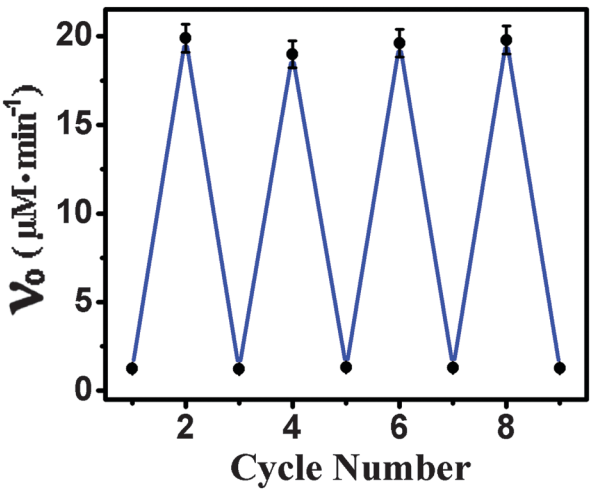

Fig. 7 Reversible switch of the catalytic activity of the GPx mimic during heating–cooling cycles between 25 °C and 37 °C. The GPx activities of supramolecular nanoenzymes were calculated from the reduction of H_2O_2 by GSH.

PNIPAM scaffold, the catalytic activity of the thermosensitive GPx mimic exhibited excellent reversibility regulated by temperature. After multiple heating–cooling cycles between 25 °C and 37 °C, the catalytic rate of the artificial GPx was still maintained steady as shown in Fig. 7. These results indicated that the formation of the vesicle-like self-assembled structure played a vital role in the regulatory functions of the catalytic behaviour of the artificial GPx.

Conclusions

In conclusion, through the amphipathic molecule multilevel self-assembly we have successfully constructed a temperature

responsive supra-amphipathic vesicle as a smart thermosensitive GPx mimic formed by the cyclodextrin-based host–guest chemistry. The catalytic activity of the GPx mimic exhibited reversibly regulated temperature-responsive characteristics. Taken as a real enzyme catalyst, we also demonstrated its typical saturation kinetics behaviour. At 25 °C, the catalytic activity of the GPx mimic was found to be 1.3 ± 0.08 (μM min^{-1}), in contrast the value rapidly increased to 19.9 ± 0.6 (μM min^{-1}) at 37 °C. The certain advantages for our research were that we achieved facile preparation by noncovalent interactions and controllable catalytic activity based on the assembly and disassembly of the vesicle structure which provided a unique microenvironment for enzymatic reaction near the body temperature. We hoped that this approach may provide an extensive way in the design of various intelligent responsive and reversible materials. Such smart GPx mimics could be endowed with feasible application prospects as antioxidant medicines in which catalytic activity can be controlled on the basis of the demand of the human body in the near future.

Acknowledgements

We are grateful to the financial support of the Natural Science Foundation of China (no. 21234004, 21420102007, 21574056, 21221063, and 21474038), the 111 project (B06009), and the Chang Jiang Scholars Program of China.

Notes and references

1 H. Sies, *Exp. Physiol.*, 1997, **82**, 291–295.
2 H. Sies, *Angew. Chem., Int. Ed. Engl.*, 1986, **25**, 1058–1071.
3 H. Sies, Oxidative Stress: Introductory Remarks, in *Oxidative Stress*, ed. H. Sies, Academic Press, London, 1985, p. 1.
4 O. Epp, R. Ladenstein and A. Wendel, *Eur. J. Biochem.*, 1983, **133**, 51–69.
5 L. Flohé, G. Loschen, W. A. Günzler and E. Eichele, *Hoppe-Seyler's Z. Physiol. Chem.*, 1972, **353**, 987–999.
6 Z. Dong, J. Liu, S. Mao, X. Huang, B. Yang, X. Ren, G. Luo and J. Shen, *J. Am. Chem. Soc.*, 2004, **126**, 16395–16404.
7 T. G. Back, D. Kuzma and M. Parvez, *J. Org. Chem.*, 2005, **70**, 9230–9236.
8 S. S. Zade, S. Panda, H. B. Singh, R. B. Sunoj and R. J. Butcher, *J. Org. Chem.*, 2005, **70**, 3693–3704.
9 X. Zhang, H. Xu, Z. Dong, Y. Wang, J. Liu and J. Shen, *J. Am. Chem. Soc.*, 2004, **126**, 10556–10557.
10 C. Zhang, T. Pan, C. Salesse, D. Zhang, L. Miao, L. Wang, Y. Gao, J. Xu, Z. Dong, Q. Luo and J. Liu, *Angew. Chem., Int. Ed.*, 2014, **53**, 13536–13539.
11 S. Mao, Z. Dong, J. Liu, X. Li, X. Liu, G. Luo and J. Shen, *J. Am. Chem. Soc.*, 2005, **127**, 11588–11589.
12 X. Liu, L. A. Silks, C. Liu, M. Ollivault-Shiflett, X. Huang, J. Li, G. Luo, Y. Hou, J. Liu and J. Shen, *Angew. Chem., Int. Ed.*, 2009, **48**, 2020–2023.
13 Y. Tang, L. Zhou, J. Li, Q. Luo, X. Huang, P. Wu, Y. Wang, J. Xu, J. Shen and J. Liu, *Angew. Chem., Int. Ed.*, 2010, **49**, 3920–3924.
14 P. Jonkheijm, P. van der Schoot, A. P. H. J. Schenning and E. W. Meijer, *Science*, 2006, **313**, 80–83.
15 G. O. Lloyd and J. W. Steed, *Nat. Chem.*, 2009, **1**, 437–442.
16 (*a*) Y. Yin, S. Jiao, C. Lang and J. Liu, *Soft Matter*, 2014, **10**, 3374–3385; (*b*) Y. Yin, S. Jiao, R. Zhang, X. Hu, Z. Shi and Z. Huang, *Soft Matter*, 2015, **11**, 5301–5312.
17 T. Shimoboji, E. Larenas, T. Fowle, S. Kulkarni, A. S. Hoffman and P. S. Stayton, *Proc. Natl. Acad. Sci. U. S. A.*, 2002, **99**, 16592–16596.
18 P. Neumann, H. Dib, A. M. Caminade and E. H. Hawkins, *Angew. Chem., Int. Ed.*, 2014, **53**, 1–5.
19 A. Piermattei, S. Karthikeyan and R. P. Sijbesma, *Nat. Chem.*, 2009, **1**, 133–137.
20 J. S. Scarpa, D. D. Mueller and I. M. Klotz, *J. Am. Chem. Soc.*, 1967, **89**, 6024–6030.
21 M. Heskins and J. E. Guillet, *J. Macromol. Sci., Part A: Pure Appl. Chem.*, 1968, **2**, 1441.
22 H. G. Schild, *Prog. Polym. Sci.*, 1992, **17**, 163–249.
23 Y. Xia, X. C. Yin, N. A. D. Burke and H. D. H. Stover, *Macromolecules*, 2005, **38**, 5937.
24 (*a*) Y. Wang, N. Ma, Z. Wang and X. Zhang, *Angew. Chem., Int. Ed.*, 2007, **46**, 2823–2826; (*b*) X. Zhang, Z. Chen and F. Würthner, *J. Am. Chem. Soc.*, 2007, **129**, 4886–4887; (*c*) N. Kimizuka, T. Kawasaki, K. Hirata and T. Kunitake, *J. Am. Chem. Soc.*, 1998, **120**, 4094–4104.
25 A. Harada, R. Kobayashi, Y. Takashima, A. Hashidzume and H. Yamaguchi, *Nat. Chem.*, 2010, **3**, 34–37.
26 O. Kretschmann, S. W. Choi, M. Miyauchi, I. Tomatsu, A. Harada and H. Ritter, *Angew. Chem., Int. Ed.*, 2006, **45**, 4361–4365.
27 C. Koopmans and H. Ritter, *Macromolecules*, 2008, **41**, 7418–7422.
28 J. Liu, G. Chen, M. Guo and M. Jiang, *Macromolecules*, 2010, **43**, 8086–8093.
29 (*a*) A. Mueller and D. F. O'Brien, *Chem. Rev.*, 2002, **102**, 727–757; (*b*) S. Zhou, C. Burger, B. Chu, M. Sawamura, N. Nagahama, M. Toganoh, U. E. Hackler, H. Isobe and E. Nakamura, *Science*, 2001, **291**, 1944–1947; (*c*) X. Zhang, S. Rehm, M. M. Safont-Sempere and F. Würthner, *Nat. Chem.*, 2009, **1**, 623–629.
30 G. Masci, L. Giacomelli and V. Crescenzi, *Macromol. Rapid Commun.*, 2004, **25**, 559–564.
31 (*a*) Z. Dong, J. Liu, S. Mao, X. Huang, B. Yang, G. Luo and J. Shen, *J. Am. Chem. Soc.*, 2004, **126**, 16395; (*b*) Z. Dong, J. Liu and S. Mao, *J. Inclusion Phenom. Macrocyclic Chem.*, 2006, **56**, 179.
32 T. M. Eggenhuisen, C. R. Becer, M. W. M. Fijten, R. Eckardt, R. Hoogenboom and U. S. Schubert, *Macromolecules*, 2008, **41**, 5132–5140.
33 S. R. Wilson, P. A. Zucker, R. R. C. Huang and A. Spector, *J. Am. Chem. Soc.*, 1989, **111**, 5936–5939.
34 C. Alexander and K. M. Shakesheff, *Adv. Mater.*, 2006, **18**, 3321–3328.

35 T. Rossow, S. Bayer, R. Albrecht, C. C. Tzschucke and S. Seiffert, *Macromol. Rapid Commun.*, 2013, **34**, 1401–1407.
36 R. Breslow and S. D. Dong, *Chem. Rev.*, 1998, **98**, 1997–2011.
37 M. V. Rekharsky and Y. Inoue, *Chem. Rev.*, 1998, **98**, 1875–1917.
38 Y. Liu and Y. Chen, *Acc. Chem. Res.*, 2006, **39**, 681–691.
39 S. Kiyonaka, K. Sugiyasu, S. Shinkai and I. Hamachi, *J. Am. Chem. Soc.*, 2002, **124**, 10954–10955.
40 Y. J. Jeon, P. K. Bharadwaj, S. Choi, J. W. Lee and K. Kim, *Angew. Chem., Int. Ed.*, 2002, **41**, 4474–4476.
41 S. A. Nepogodiev and J. F. Stoddart, *Chem. Rev.*, 1998, **98**, 1959–1976.
42 Z. Huang, Q. Luo, S. Guan, J. Gao, Y. Wang, B. Zhang, L. Wang, J. Xu, Z. Dong and J. Liu, *Soft Matter*, 2014, **10**, 9695–9701.
43 J. Li, C. Si, H. Sun, J. Zhu, T. Pan, S. Liu, Z. Dong, J. Xu, Q. Luo and J. Liu, *Chem. Commun.*, 2015, **51**, 9987–9990.
44 Y. Yin, S. Jiao, C. Lang and J. Liu, *RSC Adv.*, 2014, **4**, 25040–25050.